

[Click here to view linked References](#)

The effect of aerosol-deposited ash components on a cobalt-based Fischer-Tropsch catalyst

Ljubiša Gavrilović^{a,*}, Jan Brandin^b, Anders Holmen^a, Hilde J. Venvik^a, Rune Myrstad^c, Edd A. Blekkan^a

^a *Norwegian University of Science and Technology, Department of Chemical Engineering, Sem Sælands vei 4, 7491 Trondheim, Norway*

^b *Linnæus University, Department of Built Environment and Energy Technology, 351 95 Växjö, Sweden*

^c *SINTEF Industry, NO-7465 Trondheim, Norway*

Corresponding author: ljubisa.gavrilovic@ntnu.no

Abstract

The effect of ash salts on Co-based Fischer-Tropsch catalysts was studied using an aerosol deposition technique. The major elements in the ash were found to be K, S and Cl. The ash was deposited on a calcined catalyst as dry particles with an average diameter of approx. 350 nm. The loading of ash particles was varied by varying the time of exposure to the particles in a gas stream. Catalyst characterization did not reveal significant differences in cobalt dispersion, reducibility, surface area, pore size, or pore volume between the reference and the catalysts with ash particles deposited. Activity measurements showed that following a short exposure to the mixed ash salts (30 minutes), there were no significant loss of activity, but a minor change in selectivity of the catalyst. Extended exposure (60 minutes) led to some activity loss and changes in selectivity. However, extending the exposure time and thus the amount deposited as evidenced by elemental analysis did not lead to a further drop in activity. This behavior is different from that observed with pure potassium salts, and is suggested to be related to the larger size of the aerosol

1
2
3
4 particles deposited. The large aerosol particles used here were probably not penetrating the
5
6 catalyst bed, and to some extent formed an external layer on the catalyst bed. The ash salts are
7
8 therefore not able to penetrate to the pore structure and reach the Co active centers, but are
9
10 mixed with the catalyst and detected in the elemental analysis.
11
12
13
14

15 **1. Introduction**

16
17
18 Biomass to liquid fuels (BTL) via gasification and Fischer-Tropsch synthesis (FTS) is an attractive
19
20 process for production of liquid fuels (diesel and jet fuel)[1]. The process involves gasification of
21
22 biomass where synthesis gas (CO + H₂) is produced. Following cleaning and gas conditioning, the
23
24 synthesis gas is converted to hydrocarbons *via* the Fischer-Tropsch synthesis[2]. During biomass
25
26 gasification, the inorganic species are usually converted into bottom ash or fly ash[3]. Alkali salts
27
28 (mainly potassium) are the dominant salts in the ash composition after biomass gasification[4].
29
30 Pagels *et al.*[4] reported the formation of fine particles (around 100 nm) during biomass
31
32 combustion containing mainly the elements K, S, and Cl in the produced gas stream. It was
33
34 reported[5, 6] that potassium species (KCl and K₂SO₄) in the form of submicron aerosols can be
35
36 deposited on the external catalyst surface. Froment *et al.*[7] performed thermodynamic
37
38 equilibrium calculations during wood gasification and concluded that potassium will be semi-
39
40 volatile in the form of hydroxide, carbonate and chloride. The removal of these species from
41
42 syngas from a circulating fluid bed, down to a level where they have no influence on a cobalt-
43
44 catalysed FTS process, has been demonstrated using standard equipment such as ZnO and active
45
46 carbon filters) [6]. However, imperfections in the cleaning section or poor design can allow the
47
48 presence of these components in the produced syngas. Deactivation of Co based Fischer-Tropsch
49
50 (FT) catalyst by alkali species is known from before[8–14]. In previous communications we have
51
52
53
54
55
56
57
58
59
60
61
62
63
64
65

1
2
3
4 shown that aerosol deposition of potassium nitrate[15] or potassium salts expected to be present
5
6
7 in syngas from high-temperature gasification of biomass[16], lead to a similar deactivation of a
8
9
10 Co-based catalyst. In both cases, and similar to the results obtained using liquid phase deposition
11
12 of the salts, it is however difficult to observe any measurable change in the catalyst
13
14 characteristics following deposition. This implies that the deactivating species somehow is
15
16 transported to the active sites of the catalyst during pretreatment or reaction[9, 10, 15, 16]. In
17
18 this communication we aim to investigate the influence of impurities present in the real feed, by
19
20 collecting a sample of fly ash from burning charcoal and depositing this ash on a cobalt-based FTS
21
22 catalyst. The produced ash was expected to contain a realistic mixture of inorganic contaminants,
23
24
25 which potentially can reach the FTS catalyst in a BTL plant.
26
27
28
29

30 **2. Experimental**

31 32 33 34 2.1. Catalyst exposure by aerosol deposition of ash salts

35
36
37 The reference catalyst (20%Co/0,5%Re/ γ Al₂O₃, for the detailed description of catalyst synthesis
38
39 see[15]) was poisoned using the aerosol deposition technique. The equipment used is shown in
40
41 Fig. 1. A detailed description of apparatus is given elsewhere[17]. In short, the catalyst bed is
42
43 placed in the middle of the tubular quartz reactor inside of electrically heated oven. The lower
44
45 part of the catalyst bed consists of a glass frit, which allows the gas to pass through. The ash salt
46
47 solution was prepared by sequentially dissolving the fly ash (produced from burning charcoal) in
48
49 deionized water and then the solution was filtered several times. The produced ash solution
50
51 (8.7mg/dm³) was placed in the atomizer deposited by flowing gas through the atomizer and
52
53 through the catalyst sample. The deposition time was varied from 30 minutes, 60 minutes and
54
55
56
57
58
59
60
61
62
63
64
65

1
2
3
4 300 minutes with the corresponding sample names Ash1, Ash2 and Ash3, respectively. All the
5
6
7 deposition experiments were performed at 573K and 1 bar on calcined catalyst samples. The
8
9
10 drying time of the generated particles at these conditions is in the range of milliseconds, while
11
12 the residence time of the gas in the oven is several seconds[18].This means that the aerosol
13
14
15 particles are completely dry and the salt is transported and deposited in the form of solid particles
16
17 on the catalyst. A scanning mobility particle sizer (SMPS; TSI Inc.) consisting of a differential
18
19
20 mobility analyzer (DMA; TSI Inc. Model 3081) was used to physically characterize aerosol particles
21
22 according to their electrical mobility[17, 18]. This technique provides an estimate of the particle
23
24
25 size distribution. Inductively coupled plasma (ICP-MS) was used to determine ppm levels of ash
26
27 components. The samples (10-20 mg) were added to 1.5 ml of conc. HNO₃ in a 205 ml PFA (high-
28
29
30 purity Perfluoroalkoxy) bottle, shaking occasionally for some minutes. Ultra-purified water was
31
32
33 added, and the flask was left for approximately one hour. Then the solution was further diluted
34
35 to achieve approximately 0.1 M total acid concentration and analyzed by ICP-MS.
36
37

38 *Figure 1. Experimental setup for catalyst exposure to the aerosol particles at 573 K.*
39
40

41 2.2. Catalyst characterization

42
43
44 Volumetric adsorption of N₂ was performed on a Tristar II 3020 to determine surface area, pore
45
46
47 volume and average pore diameter of the catalyst before and after aerosol deposition. Before
48
49
50 measurement at liquid nitrogen temperature, the samples (~70mg 53-90µm) were outgassed in
51
52
53 vacuum, first at ambient temperature for 1h and then at 473 K overnight. The Brunauer-Emmet-
54
55
56 Teller (BET)[19] isotherm was used for calculation of the surface area and the Barret-Joyner-
57
58
59
60
61
62
63
64
65

1
2
3
4 Halenda (BJH)[20] method was applied to determine pore volumes and average pore diameters
5
6
7 of the samples using the desorption branch of the isotherm.
8
9

10 H₂-chemisorption was performed using a Micromeritics ASAP2010 unit. The catalyst sample (0.2
11
12 g) was loaded in the chemisorption reactor. To keep the catalyst in place for the measurement,
13
14 it was placed between quartz wool wads. Prior to chemisorption, the sample was reduced *in situ*.
15
16
17 The sample was heated with a ramping rate of 60 K/h from ambient temperature to 623 K and
18
19 kept at this temperature in flowing hydrogen for 16 h. The samples were then cooled to 313 K
20
21 under vacuum. Chemisorption data was collected at 313 K between 0.020 and 0.667 bar H₂
22
23 pressure. It was assumed that each surface cobalt atom was one H chemisorption site and that
24
25
26 neither Re, ash impurities nor the support contributed to chemisorption.
27
28
29

30
31
32 Temperature programmed reduction (TPR) experiments were performed in an Altamira AMI-
33
34 300RHP. The catalyst sample (100 mg) was loaded in a quartz u-tube reactor between wads of
35
36 quartz wool. First the catalyst was treated in inert gas at 473 K and then reduced in hydrogen
37
38 flow (7% H₂/Ar 50ml/min) to a temperature of 1173 K with a ramp rate of 10 K/min. After
39
40 reaching the final temperature, samples were cooled down to room temperature.
41
42
43

44 45 2.3 Fischer–Tropsch synthesis 46 47

48
49 Fischer–Tropsch synthesis was carried out in four parallel 10 mm ID steel tube fixed bed reactors
50
51 at 483 K, 20 bar and H₂/CO ratio of 2.1. The samples (1 g) were diluted with inert SiC (20 g) to
52
53 improve heat distribution and loaded between quartz wool wads to keep the catalyst in place.
54
55
56 To further improve heat distribution aluminium blocks were fixed around the reactors and the
57
58 reactors were placed in four separate electrical furnaces equipped with thermocouples for
59
60
61

1
2
3
4 temperature control and monitoring. After leak tests with He the pressure was kept at 1.5 bar
5
6 and flowing H₂ was introduced and the catalysts were reduced. To reach the reduction
7
8 temperature of 623 K, the samples were heated with a ramping rate of 1 K/min up to the target
9
10 temperature which was kept for 16 h. After reduction, the samples were cooled to 443 K. Before
11
12 introduction of syngas (250 Nml/min) the reactors were pressurized with He to the operating
13
14 pressure of 20 bar. The temperature program was set to increase the temperature first from 443
15
16 to 463 K with a ramping rate of 20 K/min and to the final temperature of 483 K with a ramping
17
18 rate of 5 K/min. Liquid Fischer Tropsch products, wax and other liquids (water and light
19
20 hydrocarbons), were collected in a hot trap at ~360 K and a cold trap at ambient temperature,
21
22 respectively. The light gases were analyzed using a HP 6890 gas chromatograph. H₂, N₂ (internal
23
24 standard), CO, CH₄ and CO₂ were analyzed on TCD following separation on a Carbosieve column.
25
26 Hydrocarbon products were separated with a GS-Alumina PLOT column and detected on flame
27
28 ionization detector (FID). CH₄ was used to combine TCD and FID analysis. The synthesis gas
29
30 contained 3% N₂ which served as an internal standard for quantification of the products to close
31
32 the mass balance. After ~24 h time on stream (TOS) activity data is reported based on
33
34 measurements at constant feed rate (250 Nml/min). Then the feed rate of synthesis gas was
35
36 adjusted to obtain ~50% CO conversion. Selectivity data based on the analysis of C₁–C₄
37
38 hydrocarbons in gas phase are reported after ~48 h time-on-stream (TOS) at 50 ± 5% CO
39
40 conversion. Since the focus is on the amount of higher hydrocarbons, the selectivity is reported
41
42 in the usual way as C₅+ and CH₄ selectivity.
43
44
45
46
47
48
49
50
51
52
53
54
55
56

57 **3. Results and discussion**

58
59
60
61
62
63
64
65

1
2
3
4 The generated aerosol particles from ash salts have been characterized by SMPS (in the range
5
6 ~20– 700 nm). The mass size distribution ($\mu\text{g}/\text{m}^3$) of generated ash particles is shown in Fig. 2.
7
8
9
10 The size distribution ranges from approximately 75 nm up to the cut off of the instrument range
11
12 (700 nm) with an apparent mass average size around 400 nm. This is considerably larger than the
13
14 particles formed from pure potassium salts (average diameters 200-230 nm)[16] in the same
15
16 setup. The particle size is a function of the concentration in the atomizer, and thus a consequence
17
18 of using a strong solution of ash components. The ash-salt particle size is significantly larger than
19
20 the average pore-size of the material, consequently following deposition are the ash-components
21
22 only in direct contact with the external surface of the catalyst particles.
23
24
25
26
27

28 *Figure 2.* Mass size distribution of ash produced aerosol particles
29

30 ICP-MS was used to determine the concentration of ash components on the treated catalysts.
31
32
33 The general trend is that the concentration of each element increased with increasing the
34
35 deposition time (Table 1). As it was expected potassium is the dominant element, but there are
36
37 also significant concentrations of sulfur and chlorine. This indicates that potassium salts such as
38
39 K_2SO_4 and KCl are the main components in the ash. There are also traces of other metals such as
40
41 magnesium and iron. Iron is active for the FTS, but the concentration is too low to provide any
42
43 significant catalytic activity.
44
45
46
47
48
49

50 Table 1. Concentration of ash components on the catalyst following aerosol deposition (wt
51 ppm).
52

53 Key characterization results are presented in Table 2. All the poisoned samples showed the same
54
55 dispersion (approx. 7.5%), surface area (approx. $135 \text{ m}^2/\text{g}$), pore size (approx. 13.3 nm) and pore
56
57 volume ($0.47 \text{ cm}^3/\text{g}$), all close to the values measured for the reference catalyst. This is in
58
59
60
61

1
2
3
4 agreement with previous work[16] where different potassium salts (single salts) were deposited
5
6 on the Co-based catalyst based using the same technique as applied here.
7
8
9

10 Table 2. Characterization results
11

12
13
14 The TPR profiles of poisoned and reference catalysts are presented in Fig 3. All the samples
15
16 showed almost the same profile, previously observed for alumina-supported cobalt catalysts[21].
17

18
19 The first major peak represents the transition from Co_3O_4 to CoO at around 603 K and the second
20
21 peak represents the second step of the reduction, the transition from CoO to Co at around 700
22

23
24 K. Besides the major reduction peaks, a small peak close to 500 K is observed for the reference
25
26 sample. This peak is attributed to the reduction of residual cobalt nitrate[22]. This peak is absent
27

28
29 for the poisoned catalysts, probably due to the added thermal treatment during the aerosol
30
31 deposition. There appears to be a slight reduction in the peak temperatures for the poisoned
32

33
34 samples, most prominent for the second reduction step, but the effect is very small. Previously,
35

36
37 De la Osa *et al.*[23] reported that alkali or alkaline-earth metals favor reducibility compared to
38
39 an unpromoted alumina-supported cobalt catalyst, but in their samples the alkali (1 %) was
40

41
42 impregnated on the support prior to the cobalt impregnation step, which is not the case in the
43
44 present work. To conclude, that there is no significant effect of the ash on TPR profiles which is
45

46
47 in agreement with our previously published work[16].
48
49
50

51 *Figure 3. TPR profiles of temperature vs hydrogen consumption of standard catalyst and catalysts*
52 *with different ash salt loadings*
53
54
55
56
57
58
59
60
61
62
63
64
65

1
2
3
4 Catalyst activity reported as STY (site time yield) is presented in Fig 4a. The sample with the
5
6
7 shortest exposure to the ash salts (Ash1) showed the same activity as the reference catalyst,
8
9
10 while the samples with longer exposure and higher concentrations of ash components showed a
11
12 small but significant loss in activity. The selectivities to C_{5+} , CH_4 and CO_2 are reported in Figs. 4 b),
13
14 c) and d), respectively. The selectivity towards higher hydrocarbons ($S_{C_{5+}}$, Fig 4 b)) increases with
15
16 increasing ash concentration, while the methane selectivity (S_{CH_4} , Fig. 4 c)) decreased. There was
17
18 also a clear increase in the selectivity to CO_2 , Fig 4 d). These selectivity changes are similar to
19
20 those observed previously using pure potassium salts[9, 10, 16]. The combined evidence
21
22 indicates that also in the case of aerosol deposition of mixed ash salts is there a significant effect
23
24 on the cobalt FTS catalyst, but the effect is less severe than that observed for potassium salts.
25
26
27 Zheng *et al.*[24] investigated deactivation of a commercial type $V_2O_5-WO_3-TiO_2$ Selective Catalytic
28
29 Reduction (SCR) catalyst by aerosol deposition of potassium compounds and concluded that
30
31 there was no deactivation when the catalyst was exposed to the ash salts collected from biomass
32
33 combustion, while a fast deactivation was observed when the catalyst was exposed to the pure
34
35 potassium salts (KCl, K_2SO_4). This could be linked with the physical nature of the particles, the
36
37 particles are significantly larger than those deposited from pure potassium salts, and the
38
39 transport of alkali and other species from the external surface to the internal surface of the
40
41 catalysts is probably more difficult, either because of the physical distance or that the activation
42
43 and transport of the ash components is slower due to the larger particles. This might imply that
44
45 only the finest fraction of the aerosol particles is involved in the catalyst deactivation, while the
46
47 deposits of large particles do not cause significant deactivation[25]. It is speculated that larger
48
49 particles are less harmful to the catalyst since the deposition rate is lower and since the contact
50
51
52
53
54
55
56
57
58
59
60
61
62
63
64
65

1
2
3
4 area between aerosol particles deposited on the catalyst exterior and catalyst surface, will be
5
6 lower[26].
7
8
9

10 *Figure 4. Catalytic activity reported as STY (a), selectivities to C₅₊ (b), CH₄ (c) and CO₂ (d)*
11
12

13
14 The main constituent of the ash is potassium, but the ash also contains other elements, such as
15
16 sodium, magnesium, iron, sulfur and chlorine. The concentrations of these elements is low, and
17
18 they do not appear to have a strong influence on the catalyst activity. Sulfur is however a very
19
20 strong poison, and even very small concentrations are known to have a devastating effect on the
21
22 activity. However, the concentration recorded here is not sufficient to give a detectable effect on
23
24 the activity, even if the sulfur titrated the cobalt surface. Borg *et al.* [10] demonstrated a linear
25
26 correlation between the amount of sulfur added and the decline in the activity. Approximately
27
28 300 ppm of sulfur added to the catalyst represents around 4% of the cobalt surface area assuming
29
30 the surface is titrated by sulfur. However, the selectivity changes observed here are similar to
31
32 those observed with alkali poisoning, whereas sulfur poisoning was concluded not to influence
33
34 the C₅₊ selectivity of cobalt-catalyzed FTS [10]. This indicates that the changes in activity and
35
36 selectivity observed are due to the sum of the alkali and other metallic elements deposited, and
37
38 not due to the sulfur on the samples. The absence of an effect of sulfur would indicate that the
39
40 sulfur is either stable in its deposited form (probably as a metal sulfate) on the external surface
41
42 of the catalyst, or that the sulfur is efficiently removed from the system, either during catalyst
43
44 pretreatment or in the early stages of reaction.
45
46
47
48
49
50
51
52
53
54
55

56 **4. Summary and conclusions** 57 58 59 60 61 62 63 64 65

1
2
3
4 A cobalt-based FTS catalyst was exposed to solid aerosol particles of typical biomass ash
5
6 components. The most abundant elements in the ash was potassium, sulfur and chlorine, but
7
8 there were also traces of other elements such as sodium, magnesium and iron. The
9
10 characterization revealed no significant differences in dispersion, reducibility, surface area, pore
11
12 size or pore volume. The FTS activity was slightly reduced, and the selectivity altered in the same
13
14 direction as observed with pure potassium salts, indicating that deactivating species somehow is
15
16 transported to the cobalt surface, similar to the effect observed previously with pure potassium
17
18 salts deposited in the same manner or introduced via liquid impregnation.
19
20
21
22
23
24

25 **Acknowledgements**

26
27 Financial support from The Research Council of Norway under contract no. 228741 is gratefully
28
29 acknowledged.
30
31
32
33

34 **References**

- 35
36
37
38
39 1. Van Steen E, Claeys M (2008) Fischer-Tropsch catalysts for the biomass-to-liquid process. Chem.
40
41 Eng. Technol. 31:655–666
42
43
44 2. Serrano-Ruiz JC, Dumesic JA (2011) Catalytic routes for the conversion of biomass into liquid
45
46 hydrocarbon transportation fuels. Energy Environ Sci 4:83–99 .
47
48
49
50 3. Huber GW, Iborra S, Corma A (2006) Synthesis of transportation fuels from biomass: Chemistry,
51
52 catalysts, and engineering. Chem. Rev. 106:4044–4098
53
54
55
56 4. Pagels J, Strand M, Rissler J, Szpila A, Gudmundsson A, Bohgard M, Lillieblad L, Sanati M,
57
58 Swietlicki E (2003) Characteristics of aerosol particles formed during grate combustion of moist
59
60
61
62
63
64
65

- 1
2
3
4 forest residue. *J Aerosol Sci* 34:1043–1059
5
6
7
8 5. Christensen KA, Livbjerg H (1996) A Field Study of Submicron Particles from the Combustion of
9
10 Straw. *Aerosol Sci Technol* 25:185–199 .
11
12
13 6. Christensen KA, Stenholm M, Livbjerg H (1998) The formation of submicron aerosol particles, HCl
14
15 and SO₂ in straw-fired boilers. *J Aerosol Sci* 29:421–444 .
16
17
18 7. Froment K, Defoort F, Bertrand C, Seiler JM, Berjonneau J, Poirier J (2013) Thermodynamic
19
20 equilibrium calculations of the volatilization and condensation of inorganics during wood
21
22 gasification. *Fuel* 107:269–281 .
23
24
25
26 8. Tsakoumis NE, Rønning M, Borg Ø, Rytter E, Holmen A (2010) Deactivation of cobalt based
27
28 Fischer-Tropsch catalysts: A review. *Catalysis Today*. 154:162–182
29
30
31
32 9. Balonek CM, Lillebø AH, Rane S, Rytter E, Schmidt LD, Holmen A (2010) Effect of alkali metal
33
34 impurities on Co-Re catalysts for Fischer-Tropsch synthesis from biomass-derived syngas. *Catal*
35
36 *Letters* 138:8–13
37
38
39
40 10. Lillebø AH, Patanou E, Yang J, Blekkan EA, Holmen A (2013) The effect of alkali and alkaline earth
41
42 elements on cobalt based Fischer-Tropsch catalysts. *Catalysis Today*. 215:60–66
43
44
45
46 11. Borg Ø, Hammer N, Enger BC, Myrstad R, Lindvg OA, Eri S, Skagseth TH, Rytter E (2011) Effect of
47
48 biomass-derived synthesis gas impurity elements on cobalt Fischer-Tropsch catalyst performance
49
50 including in situ sulphur and nitrogen addition. *J Catal* 279:163–173
51
52
53
54 12. Forzatti P, Lietti L (1999) Catalyst deactivation. *Catal Today* 52:165–181
55
56
57
58 13. Bartholomew CH (2001) Mechanisms of catalyst deactivation. *Appl Catal A Gen* 212:17–60
59
60
61
62
63
64
65

- 1
2
3
4 14. Lillebø AH, Holmen A, Enger BC, Blekkan EA (2012) Fischer-Tropsch Conversion of Biomass-
5
6 Derived Synthesis Gas to Liquid Fuels. WIREs Energy and Environment. 2:507-524
7
8
- 9
10 15. Gavrilović L, Brandin J, Holmen A, Venvik HJ, Myrstad R, Blekkan EA (2018) Fischer-Tropsch
11
12 Synthesis – investigation of the deactivation of a Co catalyst by exposure to aerosol particles of
13
14 potassium salt. Appl Catal B Environ. 230:203–209
15
16
- 17
18 16. Gavrilović L, Brandin J, Holmen A, Venvik HJ, Myrstad R, Blekkan EA (2018) Deactivation of Co-
19
20 Based Fischer–Tropsch Catalyst by Aerosol Deposition of Potassium Salts. Ind Eng Chem Res
21
22 57:1935–1942 .
23
24
- 25
26 17. Einvall J, Albertazzi S, Hulteberg C, Malik A, Basile F, Larsson AC, Brandin J, Sanati M (2007)
27
28 Investigation of reforming catalyst deactivation by exposure to fly ash from biomass gasification
29
30 in laboratory scale. Energy and Fuels 21:2481–2488
31
32
- 33
34 18. Hinds WC (2012) Aerosol technology: properties, behavior, and measurement of airborne
35
36 particles. John Wiley & Sons
37
38
- 39
40 19. Brunauer S, Emmett PH, Teller E (1938) Adsorption of Gases in Multimolecular Layers. J Am Chem
41
42 Soc 60:309–319
43
44
- 45
46 20. Barrett EP, Joyner LG, Halenda PP (1951) The Determination of Pore Volume and Area
47
48 Distributions in Porous Substances. I. Computations from Nitrogen Isotherms. J Am Chem Soc
49
50 73:373–380
51
52
- 53
54 21. Rønning M, Tsakoumis NE, Voronov A, Johnsen RE, Norby P, Van Beek W, Borg Ø, Rytter E,
55
56 Holmen A (2010) Combined XRD and XANES studies of a Re-promoted Co/Re-Al₂O₃ catalyst at
57
58 Fischer-Tropsch synthesis conditions. Catal Today 155:289–295
59
60
61
62
63
64
65

- 1
2
3
4
5
6
7
8
9
10
11
12
13
14
15
16
17
18
19
20
21
22
23
24
25
26
27
28
29
30
31
32
33
34
35
36
37
38
39
40
41
42
43
44
45
46
47
48
49
50
51
52
53
54
55
56
57
58
59
60
61
62
63
64
65
22. Bao A, Li J, Zhang Y (2010) Effect of barium on reducibility and activity for cobalt-based Fischer-Tropsch synthesis catalysts. *J Nat Gas Chem* 19:622–627
 23. De La Osa AR, De Lucas A, Valverde JL, Romero A, Monteagudo I, Coca P, Sánchez P (2011) Influence of alkali promoters on synthetic diesel production over Co catalyst. *Catalysis Today*. 167:96–106
 24. Zheng Y, Jensen AD, Johnsson JE, Thøgersen JR (2008) Deactivation of V₂O₅-WO₃-TiO₂SCR catalyst at biomass fired power plants: Elucidation of mechanisms by lab- and pilot-scale experiments. *Appl Catal B Environ* 83:186–194 .
 25. Zheng Y, Jensen AD, Johnsson JE (2005) Deactivation of V₂O₅-WO₃-TiO₂SCR catalyst at a biomass-fired combined heat and power plant. *Appl Catal B Environ* 60:253–264 .
 26. Olsen BK, Kügler F, Castellino F, Jensen AD (2016) Poisoning of vanadia based SCR catalysts by potassium: Influence of catalyst composition and potassium mobility. *Catal Sci Technol* 6:2249–2260 .

Figure 1. Experimental setup for catalyst exposure to the aerosol particles at 573 K.

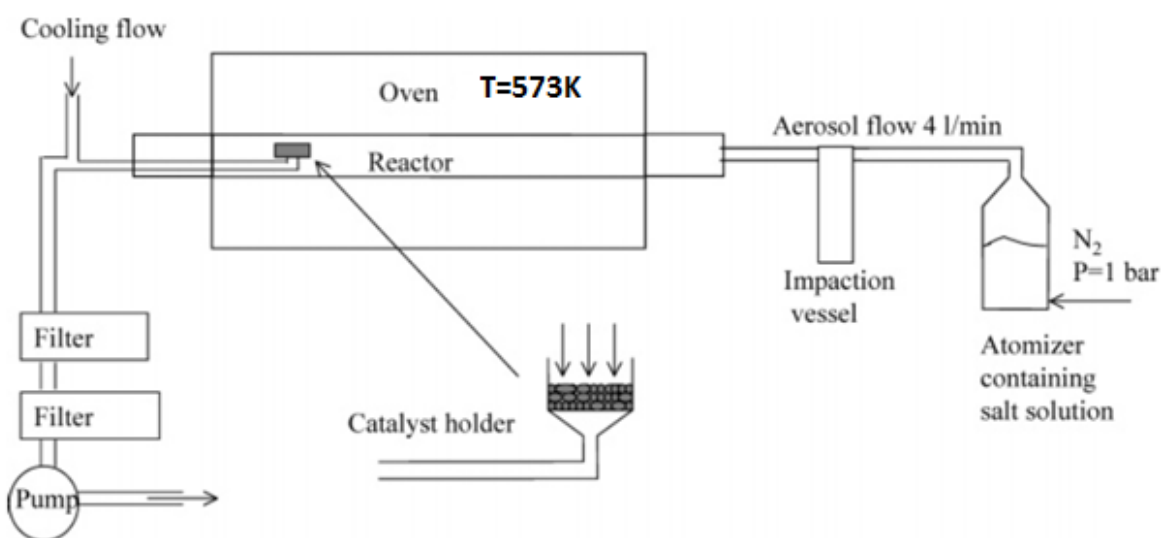


Figure 2. Mass size distribution of ash produced aerosol particles

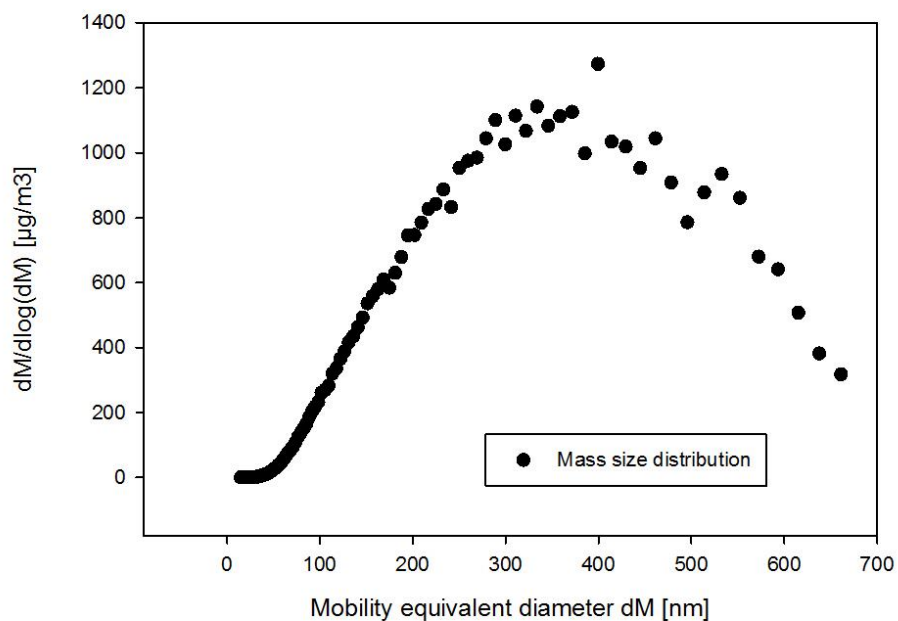


Figure 3. TPR profiles of temperature vs hydrogen consumption of standard catalyst and catalysts with different ash salt loadings

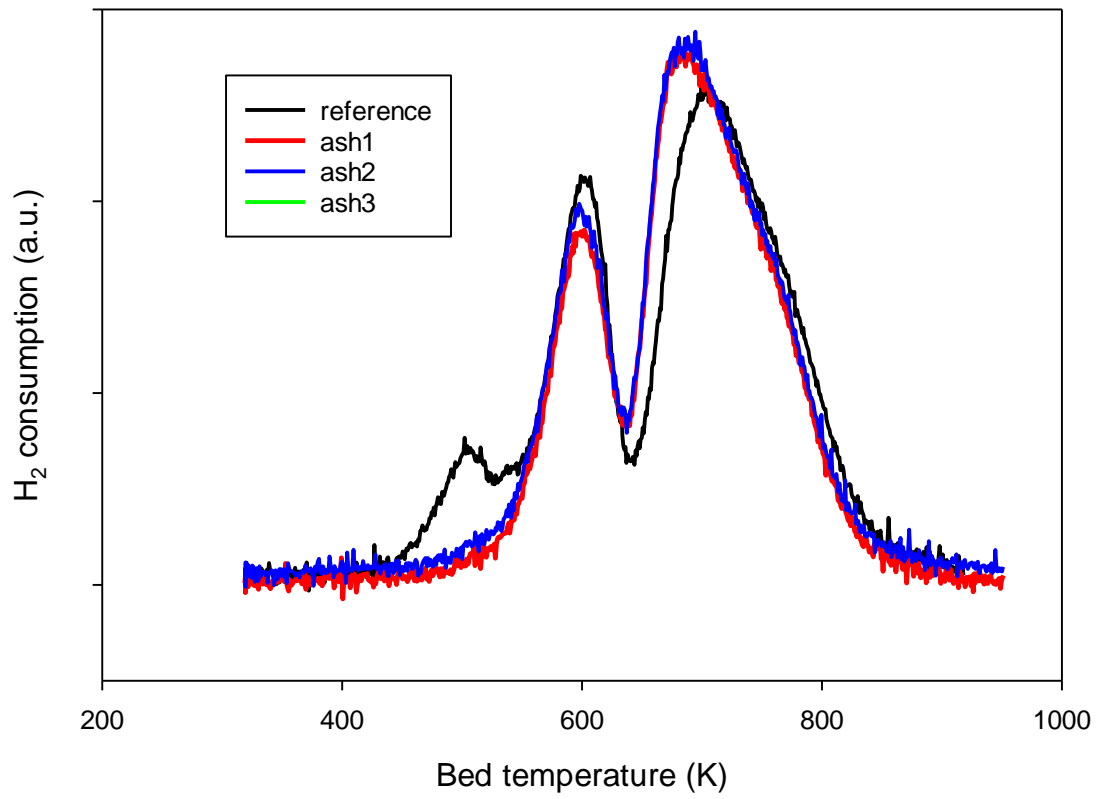


Figure 1. Catalytic activity reported as STY (a), selectivities to C_{5+} (b), CH_4 (c) and CO_2 (d)

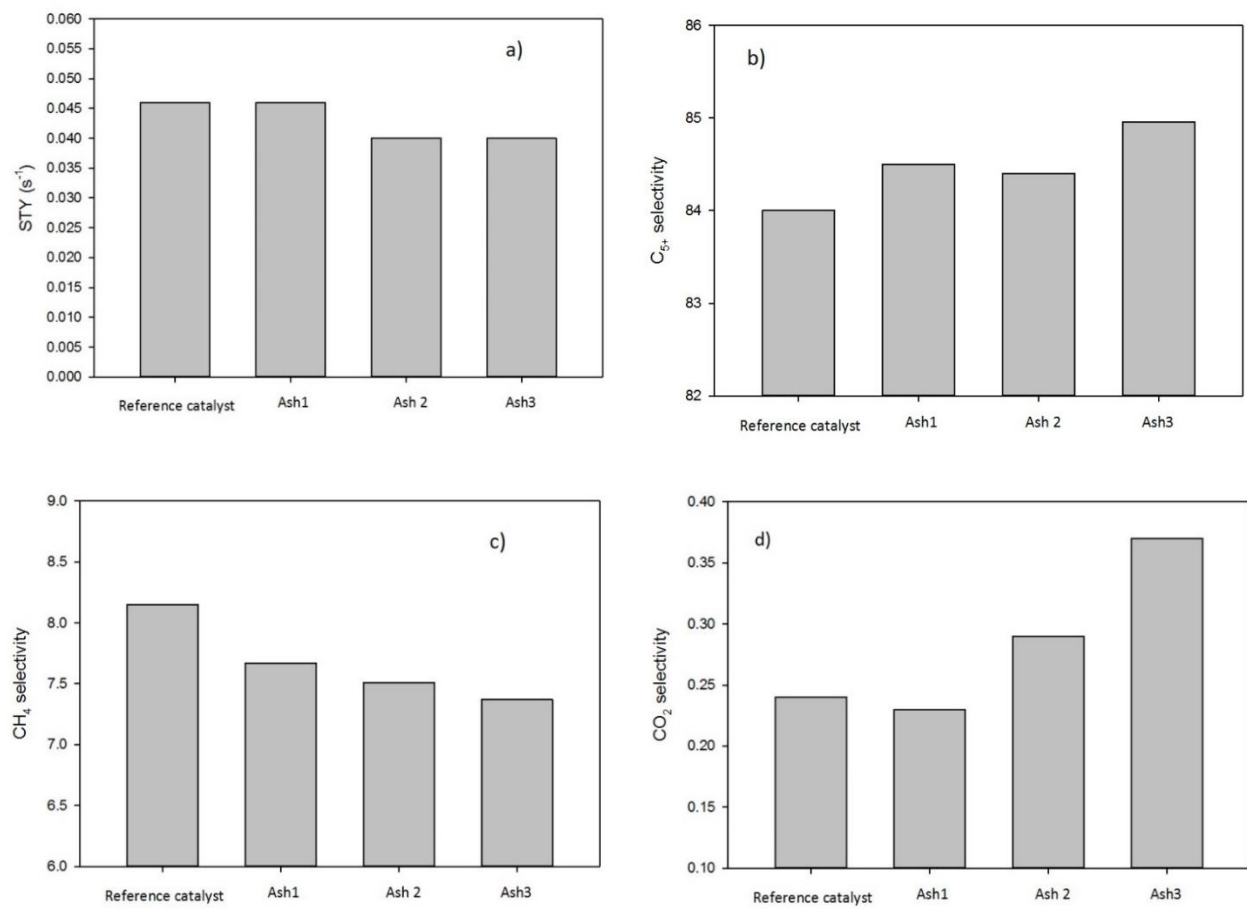
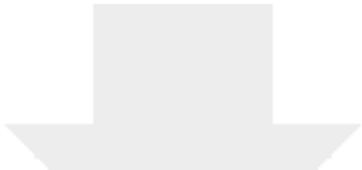


Table 1. Concentration of ash components on the catalyst following aerosol deposition (wt ppm).

element	Ash1 (ppm)	Ash2 (ppm)	Ash3 (ppm)
K	233	520	1677
Na	59	46	148
Mg	28	38	61
S	293	200	359
Cl	214	328	600
Ca	13	45	45
Fe	61	66	116

Table 2. Characterization results

Salt impurity	Dispersion (%)	Bet surface area (m ² /g)	Pore volume (cm ³ /g)	Pore size (nm)	Reduction temperature (K)	
					Co ₃ O ₄ →CoO	CoO→Co
None	7,6	133	0,45	13,1	603	704
Ash1	7,5	135	0,47	13,2	601	683
Ash2	7,1	134	0,47	13,3	598	685
Ash3	7,9	132	0,47	13,4	595	673



Click here to access/download
Supplementary Material
Cover letter.docx

